

Efficacy of Magnetotelluric Method in Delineating Structural Traps Hosting Groundwater Bodies

Akinde, A. S.

Exploration Unit, Slyvopetro International Limited. Abuja F.C.T

Afuwai, C. G.

Department of Physics, Kaduna State University, Kaduna, Nigeria

Email: slyvoakinde@yahoo.co.uk

Gata, Thomas Bulus

Department of Mineral and Petroleum Resource Engineering Technology,

Federal Polytechnic Ekowe, Bayelsa State, Nigeria.

Email: tomgata2000@gmail.com

ABSTRACT

The objectives of this study are to delimit the lateral extent, thickness and depth extent of the overburden or regolith using geophysical methods; and to determine the depth to possible structural traps hosting groundwater bodies or aquifer and fractured zone and drill depth present within the studied area. The Rock Strength Analysis, Water Quantum, Water Quality, Salinity, permeability Factor and GPS coordinates, number of structural trap/fracture sources, and Total drill depth (BHD), all in percentage, were estimated. The magnetotelluric (MT) method was deployed to infer the conductivity of the subsurface geology and as an effective tool for prospecting for groundwater potential. Geophinex, as an automatic groundwater detector, is based on the electromagnetic field principle and thus was carried out across the suspected and known strike of the conductive zone.

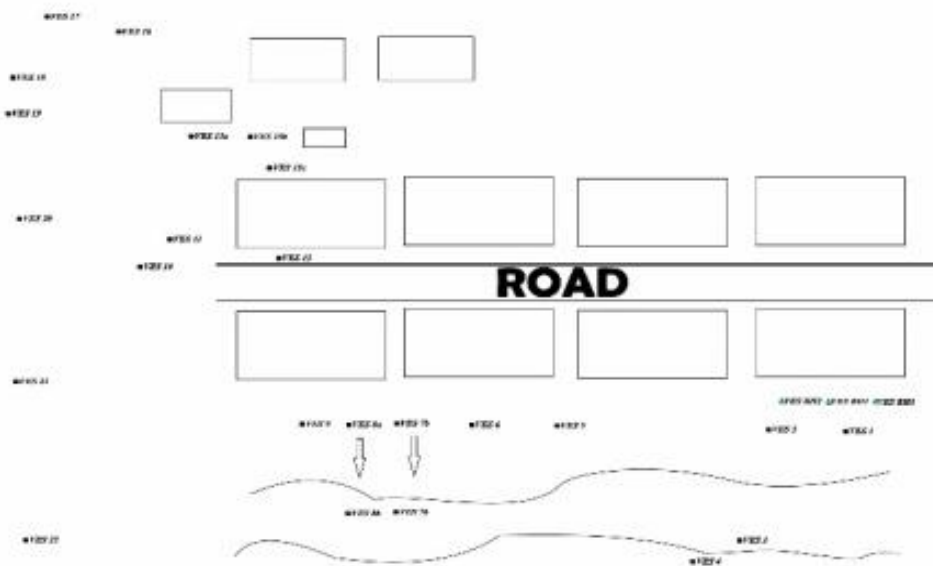
Keywords: *Geophinex. Delineation. Salinity. , North Central Nigeria*

INTRODUCTION

Locating structural traps capable of hosting underground water bodies by conventional geophysical methods has become challenging in some complex geological terrain. The efficacy of Magnetotelluric (MT) of electromagnetic source improves geophysical devices called Geophinex now play an increasingly important role in the search for

groundwater potentials in all geological terrains across the globe, including Nigeria. Offodile (1992) described the geology and geomorphology of Abuja to have been underlain by crystalline basement rocks, and it consists of rock types which contain different textures of granites, coarse to fine, consisting essentially of biotite, feldspars and quartz. In most cases, the rocks have weathered into reddish micaceous sandy-clay to clay materials capped by laterites. (Offodile, 1992). Generally, only a small amount of water can be obtained in the freshly unfractured bedrock below the weathered layers. Groundwater is found mainly in the variable weathered/transition zone, which consists of fractures, joints and cracks of the crystalline basement (Offodile 1992). Alan and Alan (2012) described the mathematical representation of field data acquisition modelling and geological interpretation.

TRINITY ESTATE KARU ABUJA



METHOD AND DISCUSSION

Concepts of Apparent Resistivity and Sounding

Magnetotelluric (MT) is a remote sensing technique that can image the earth's electrical resistivity structure from depths of a few 100 metres to several 100 kilometres. Natural electromagnetic (EM) waves are generated in the Earth's atmosphere and magnetosphere by a range of physical mechanisms.

The magnetotelluric (MT) method measures the Earth's natural electromagnetic field used as a source field. The receivers record the horizontal and mutually orthogonal components of electric and magnetic fields on the surface of the Earth. The variations in amplitude and phase of the received signals can be interpreted in terms of the resistivity structure of the subsurface or near-surface of the Earth's interior using the magnetotelluric impedance, Z . As was the case with the various DC methods, it is common practice to define an apparent resistivity in terms of measurements made over an ideally uniform earth. And, as in the case of DC methods, it is common practice to speak of a sounding, or determination of apparent resistivity as a function of depth in the earth. In contrast to the DC methods, where the spacing between electrodes was used as the depth-related measurement, in the magnetotelluric method, the frequency, or more exactly the period, of oscillations comprising the natural electromagnetic field is used as the depth-related measurement. Because of this difference in concept, soundings made with the MT method are termed *parametric*, while DC soundings are termed *geometric*.

If the earth is uniform in electrical character, the expression for impedance
Then we have

$$Z = \omega \mu_0 / k_1, \quad 1$$

For the case of a uniform earth, the layered earth correction factor, R_1 , is exactly unity. This last equation can be solved directly for the electrical resistivity (or its inverse, the electrical conductivity) by using the definition for k_1 :

$$k_1 = (i\omega \mu_0 / \rho_1)^{1/2}. \quad 2$$

The result is

$$\rho_1 = 1 / \omega \mu_0 |Z|^2. \quad 3$$

This resulting to generate Tikhonov-Cagniard formula for apparent resistivity computed from impedance measurements at the surface of the earth. Provided the earth were perfectly uniform, the formula would generate the correct value for the resistivity. If the earth is otherwise not uniform, the calculation of apparent resistivity is still possible, but it defines only an apparent resistivity loosely related to the actual resistivity distribution in the earth. This relationship can be a meaningful one, as in the case of a simply structured earth

The basic physics is illustrated below.

These EM waves travel downwards (blue) to the Earth's surface and most of the energy is reflected upwards (red). Some energy enters the Earth and diffuses downwards. The depth of penetration in the Earth is controlled by the skin depth phenomenon. The depth of penetration decreases as the EM signal frequency increases.

By measuring the horizontal electric and magnetic fields at the Earth's surface, and then going through some torturous mathematics, we can measure the electrical resistivity of the Earth as a function of depth.

Oliver Ritter *et al.* (1998) described the robust estimate nature of the relativity of magnetotelluric and geomagnetic response function. The EM signals at different frequencies originate through the following mechanisms:

- i. High-frequency signals originate in lightning activity ($f > 1$ Hz)
- ii. Intermediate frequency signals come from ionospheric resonances ($1 \text{ Hz} > f > 0.01$ Hz)
- iii. Low-frequency signals are generated by variations in the solar wind ($0.1 \text{ Hz} > f > 0.00001$ Hz)

The electrical resistivity can then be interpreted, guided by resistivity measurements made in the laboratory and other field observations, such as surficial geology. In general, rocks containing fluids such as water will have a low resistivity. Similarly, dry and cold rocks will have high resistivities.

Data Presentation and Interpretation

A total of twenty-six MT Sounding points were proposed for the study and they were thoroughly investigated and critically studied. Characteristics: depth sounding 1D curve of depth versus frequency, 2D Earth depth profile, 2D Earth latitude-Longitude profile and 3D Surface – Depth.

Frequencies were generated during the data processing, which makes the interpretation robust and result-oriented. These results are shown in Figures 4.2-4.5)a-y. The curves were interpreted quantitatively and qualitatively using Geophinex software.

Robust results were generated as shown in table 4,1.

The work done by Akinde A.S. *et al.* (2019) focused on the Ifewara shear zone/fault zone as indicated by the overprint 'Mylonite'. The research further discussed how *faults* formed from the effect of brittle rock failure and shear motion.

The interpreted results indicate distinctive structural traps hosting underground water.

3D Mapping:Surface-Depth-Frequency

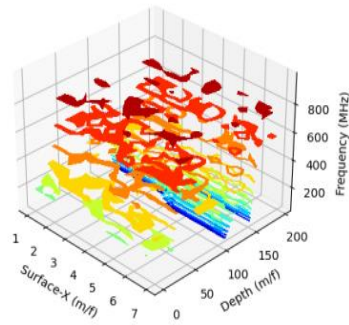


Figure 4.2a: 3D Mapping: Surface - Depth –Frequency

Earth Depth Profile

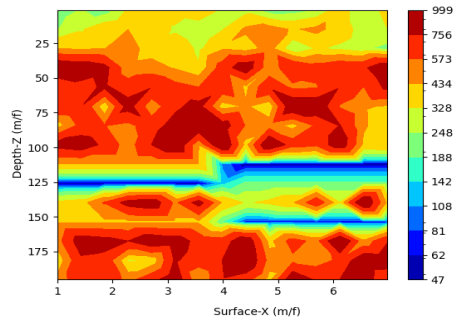


Figure 4.3a: Earth Depth Profile

Earth Lat-Long Profile

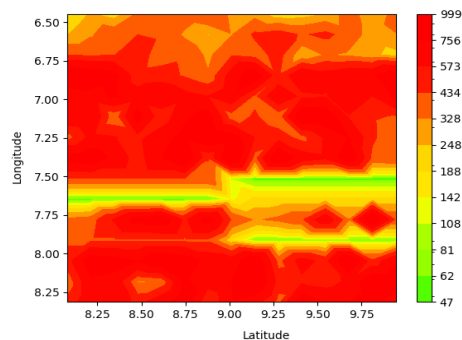


Figure 4.4a: Earth Latitude-Longitude Profile

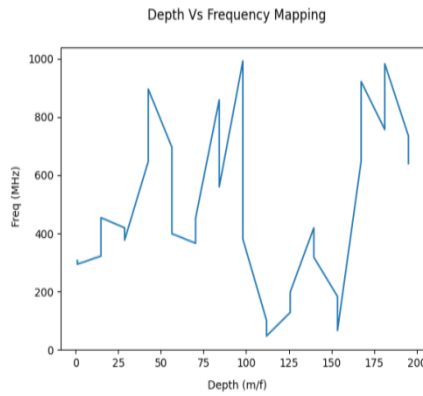


Figure 4.5a: Depth versus Frequency Mapping

3D Mapping:Surface-Depth-Frequency

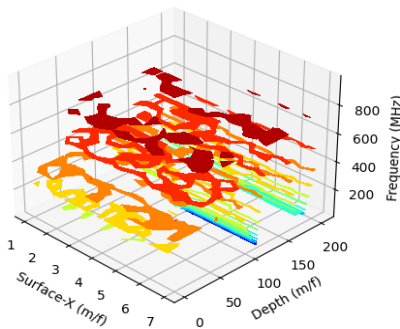


Figure 4.2b: 3D Mapping: Surface-Depth-Frequency

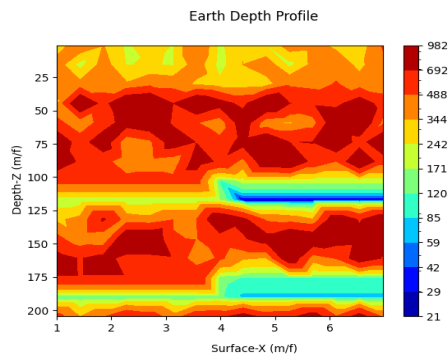


Figure 4.3b: Earth Depth Profile

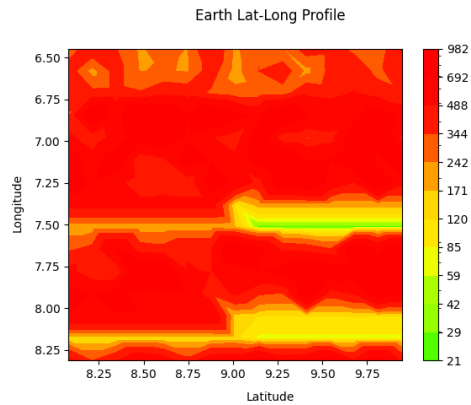


Figure 4.4b: Earth Latitude-Longitude Profile

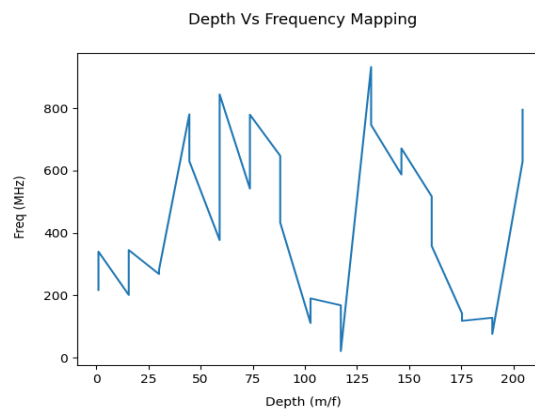


Figure 4.5b: Depth versus Frequency Mapping

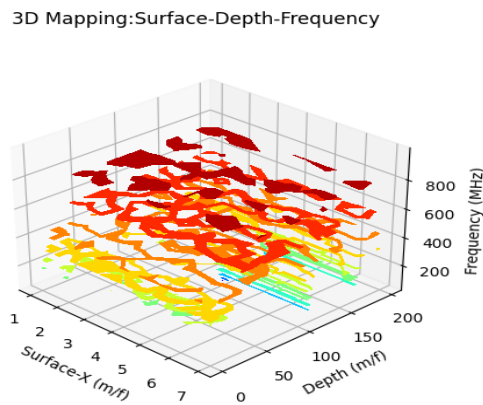


Figure 4.2c: 3D Mapping: Surface-Depth-Frequency

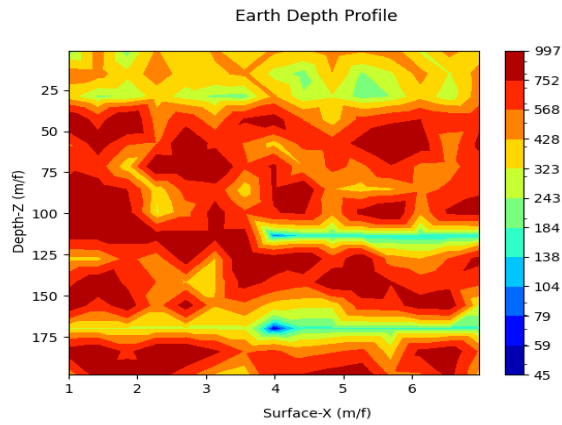


Figure 4.3c: Earth Depth Profile

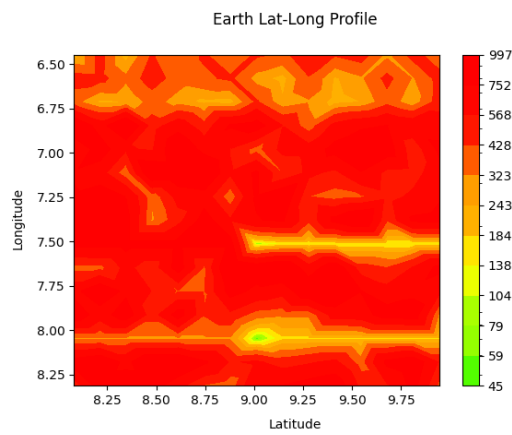


Figure 4.4c: Earth Latitude-Longitude Profile

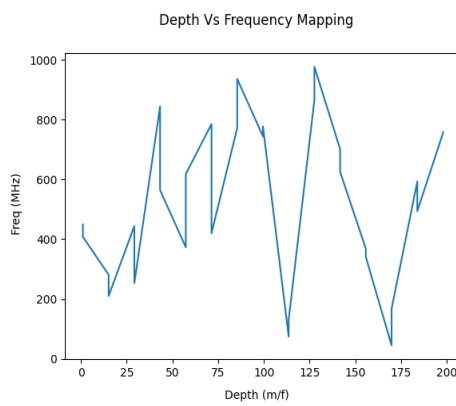


Figure 4.5c: Depth versus Frequency Mapping

3D Mapping:Surface-Depth-Frequency

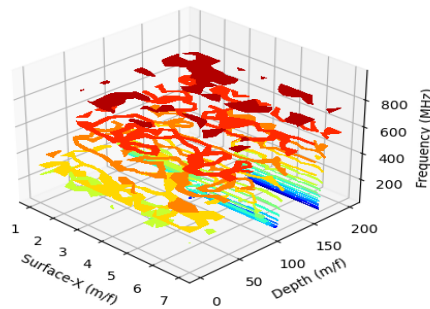


Figure 4.2d: 3D Mapping: Surface - Depth -Frequency

Earth Depth Profile

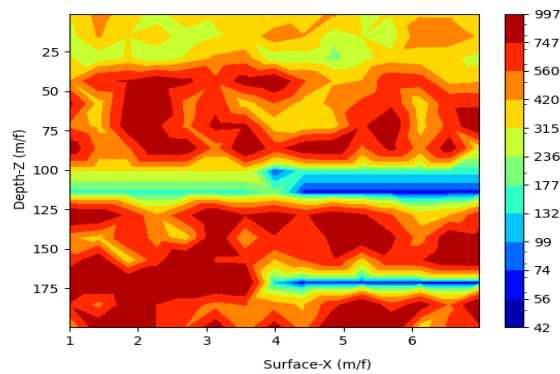


Figure 4.3d: Earth Depth Profile

Earth Lat-Long Profile

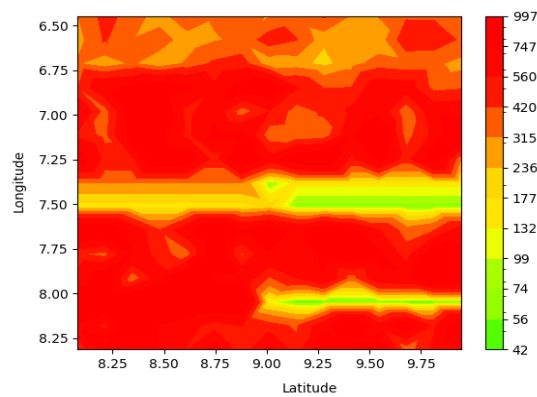


Figure 4.4d: Earth Latitude-Longitude Profile

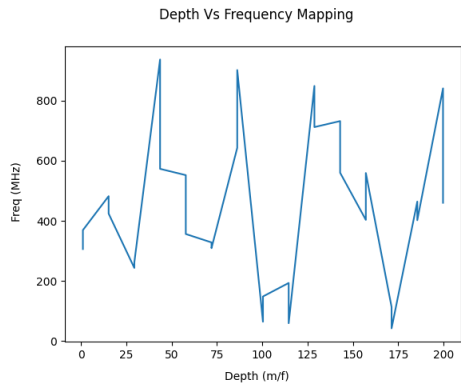


Figure 4.5d: Depth versus Frequency Mapping

3D Mapping:Surface-Depth-Frequency

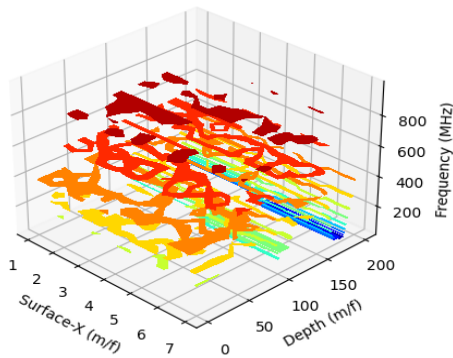


Figure 4.2e: 3D Mapping: Surface - Depth -Frequency

Earth Depth Profile

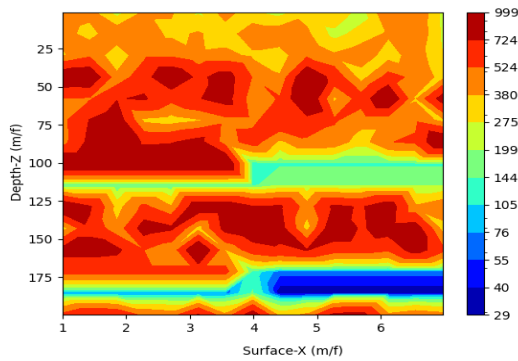


Figure 4.3e: Earth Depth Profile



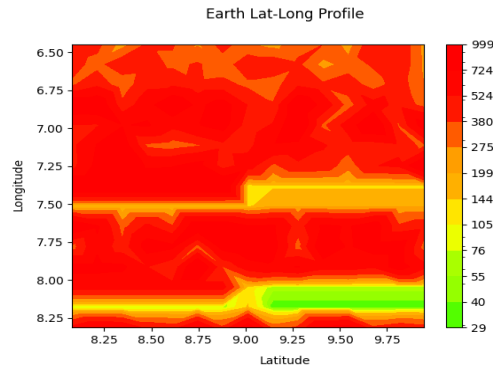


Figure 4.4e: Earth Latitude-Longitude Profile

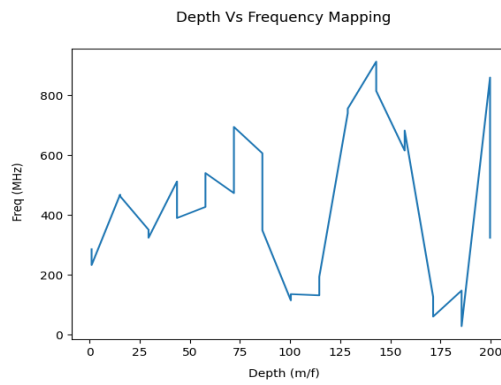


Figure 4.5e: Depth versus Frequency Mapping

3D Mapping:Surface-Depth-Frequency

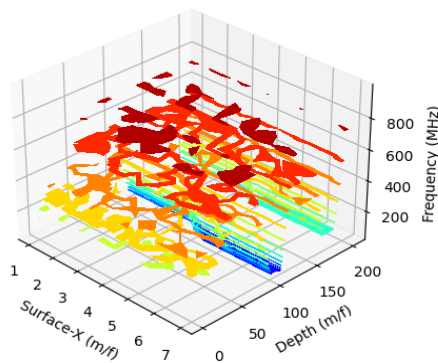


Figure 4.2f: 3D Mapping: Surface - Depth –Frequency

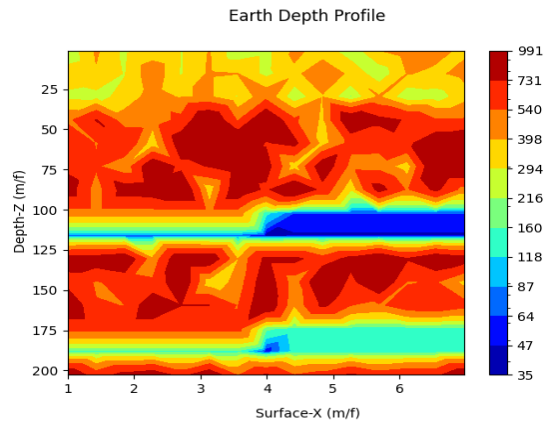


Figure 4.3f: Earth Depth Profile

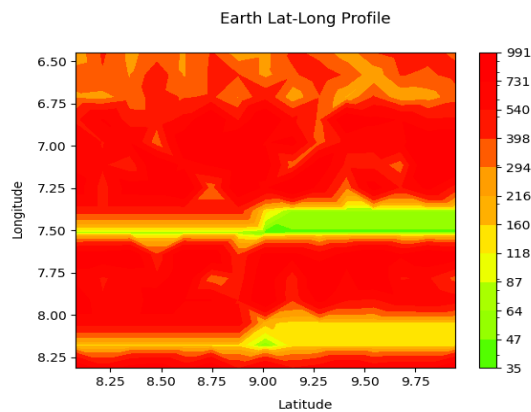


Figure 4.4f: Earth Latitude-Longitude Profile

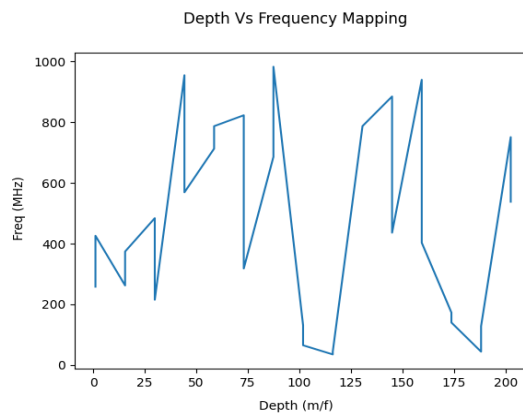


Figure 4.5f: Depth versus Frequency Mapping

3D Mapping:Surface-Depth-Frequency

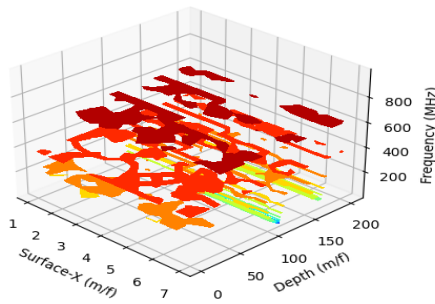


Figure 4.2g: 3D Mapping: Surface - Depth –Frequency

Earth Depth Profile

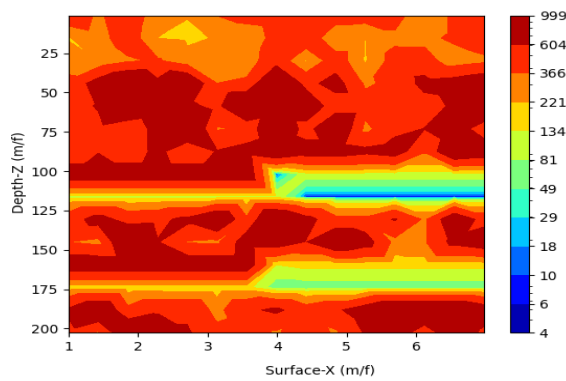


Figure 4.3g: Earth Depth Profile

Earth Lat-Long Profile

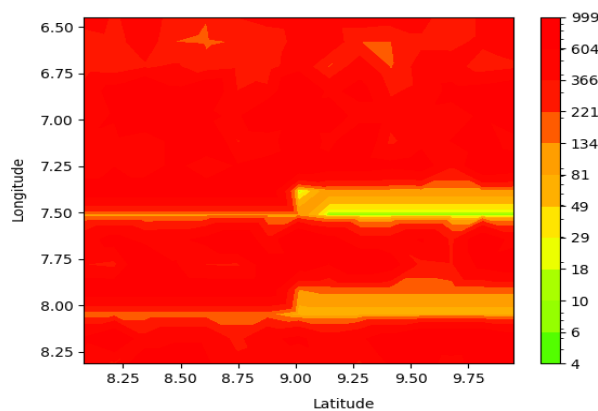


Figure 4.4g: Earth Latitude-Longitude Profile



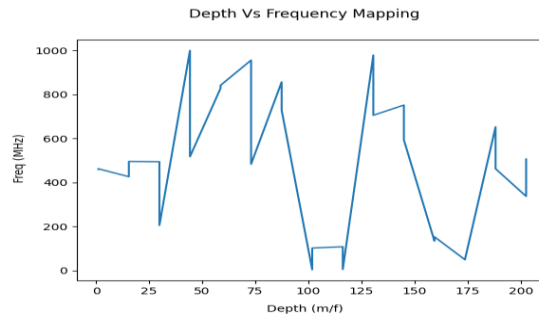


Figure 4.5g: Depth versus Frequency Mapping

3D Mapping:Surface-Depth-Frequency

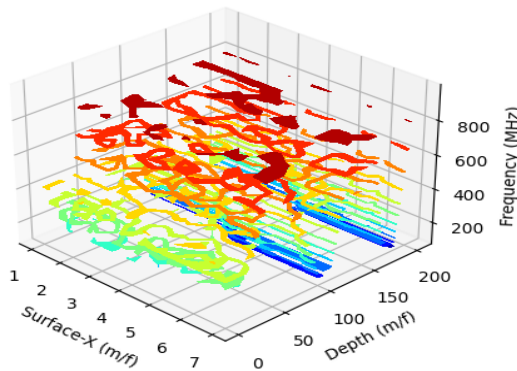


Figure 4.2h: 3D Mapping: Surface-Depth-Frequency 7 New

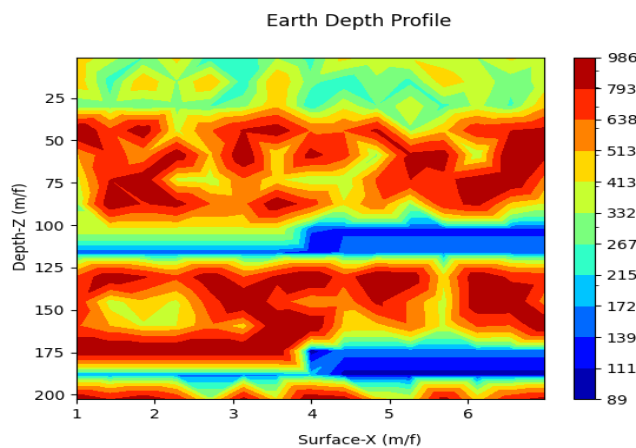


Figure 4.3h: Earth Depth Profile 7 New

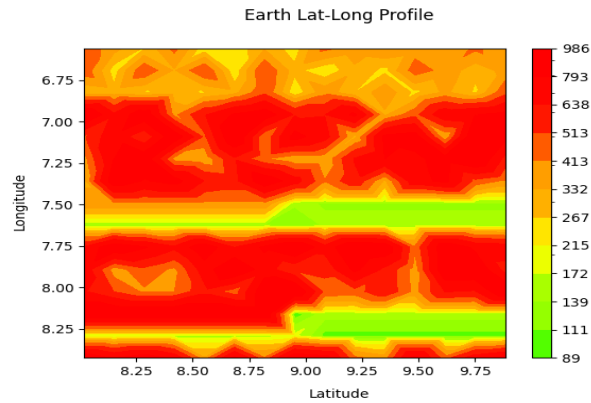


Figure 4.4h: Earth Latitude-Longitude Profile 7 New

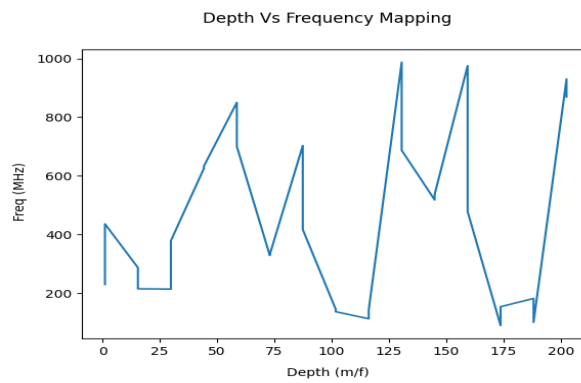


Figure 4.5h: Depth versus Frequency Mapping

3D Mapping:Surface-Depth-Frequency

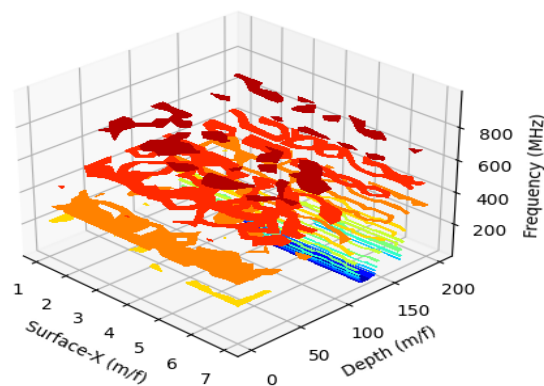
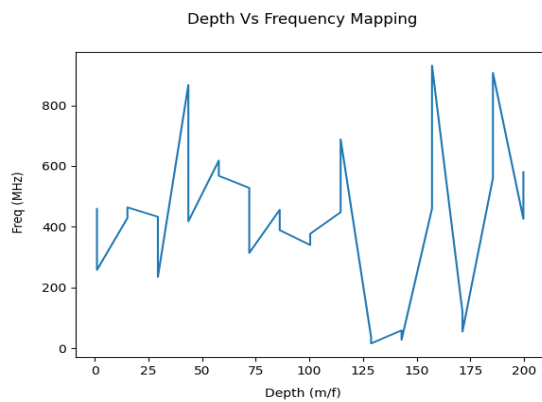
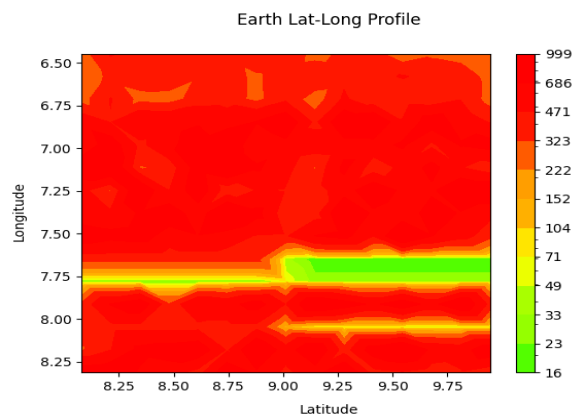
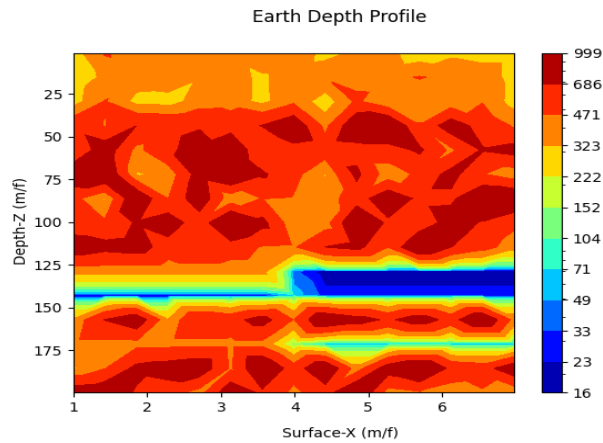


Figure 4.2i: 3D Mapping: Surface-Depth-Frequency



3D Mapping:Surface-Depth-Frequency

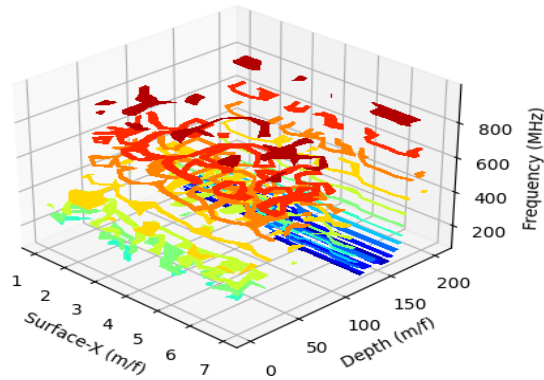


Figure 4.2j: 3D Mapping: Surface-Depth-Frequency 8 New

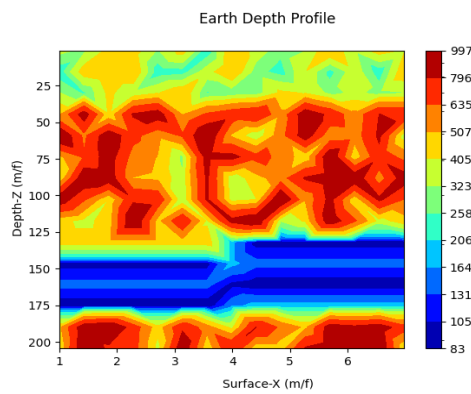


Figure 4.3j: Earth Depth Profile 8 New

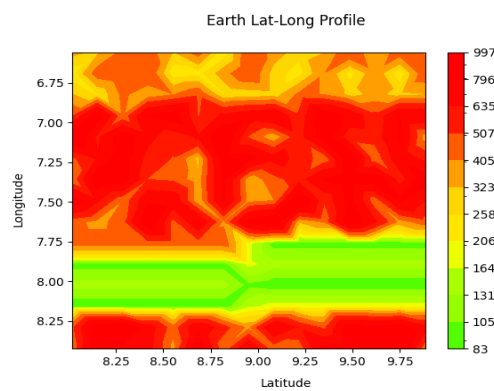


Figure 4.4j: Earth Latitude-Longitude Profile 8 New

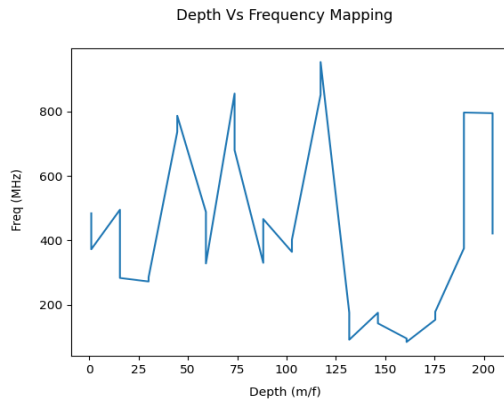


Figure 4.5j: Depth versus Frequency Mapping 8 New

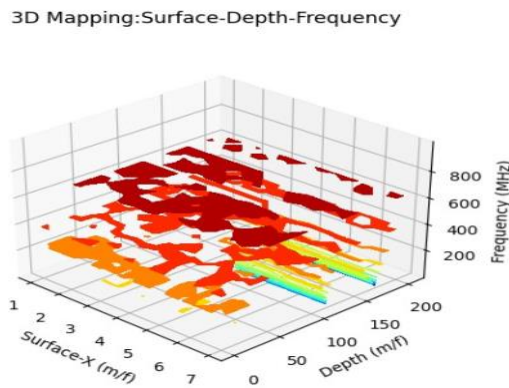


Figure 4.2k: 3D Mapping: Surface-Depth -Frequency

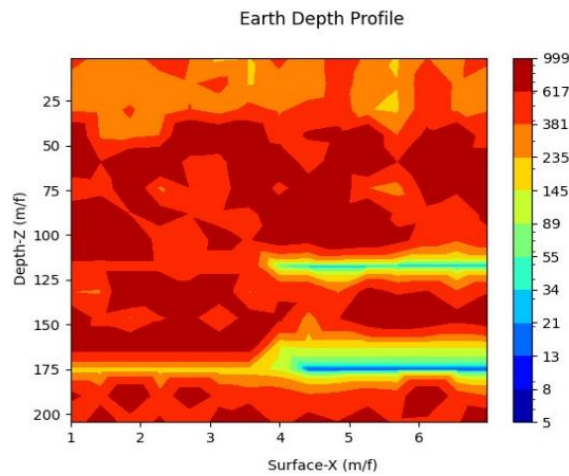


Figure 4.3k: Earth Depth Profile

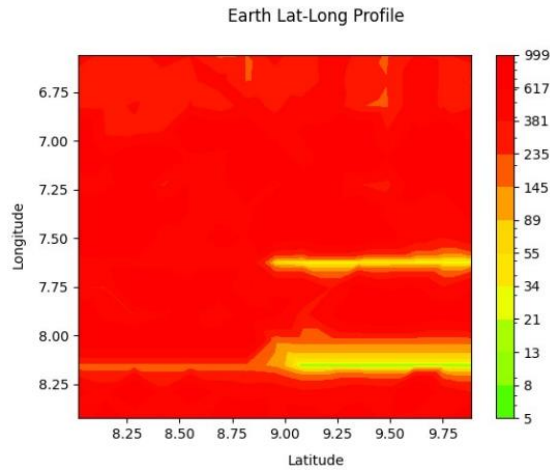


Figure 4.4k: Earth Latitude-Longitude Profile

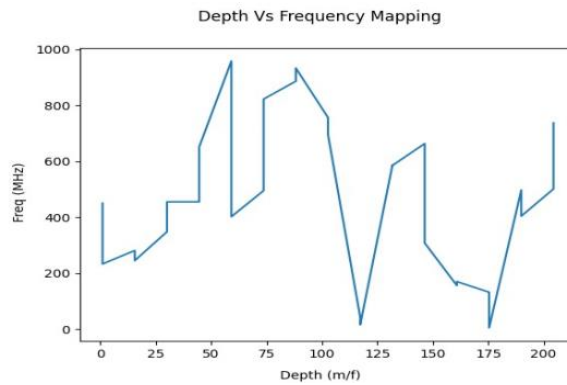


Figure 4.5k: Depth versus Frequency Mapping

3D Mapping:Surface-Depth-Frequency

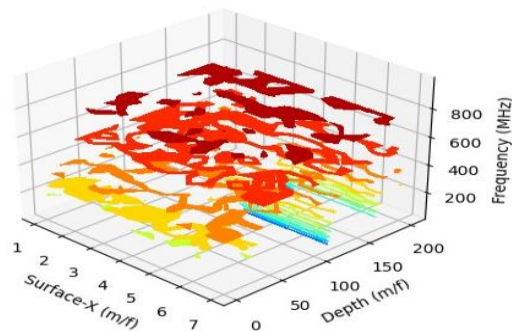


Figure 4.2l: 3D Mapping: Surface - Depth -Frequency

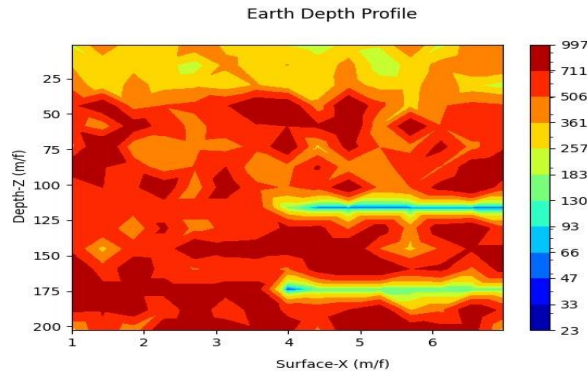


Figure 4.3l: Earth Depth Profile

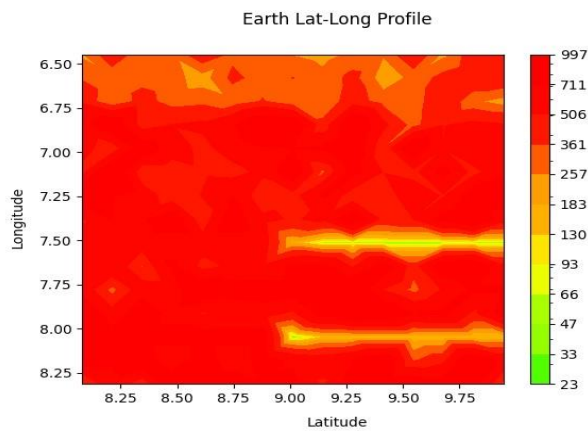


Figure 4.4l: Earth Latitude-Longitude Profile

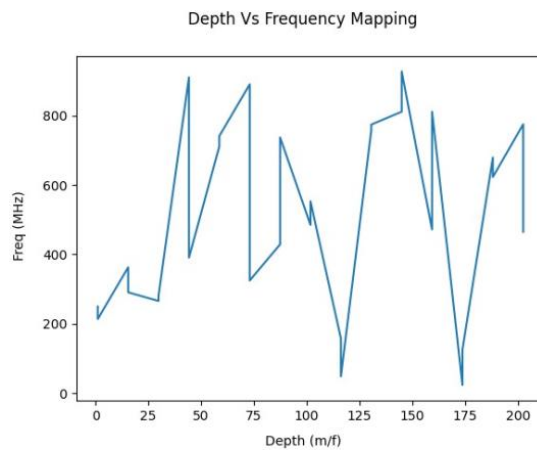


Figure 4.5l: Depth versus Frequency Mapping

3D Mapping:Surface-Depth-Frequency

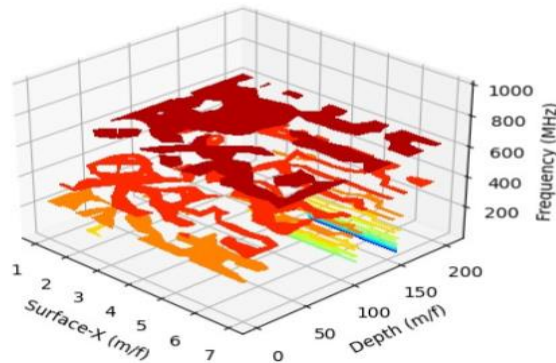


Figure 4.2m: showing 3D Mapping: Surface - Depth -Frequency

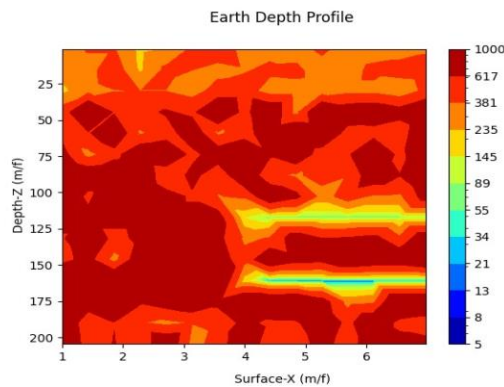


Figure 4.3m: showing Earth Depth Profile

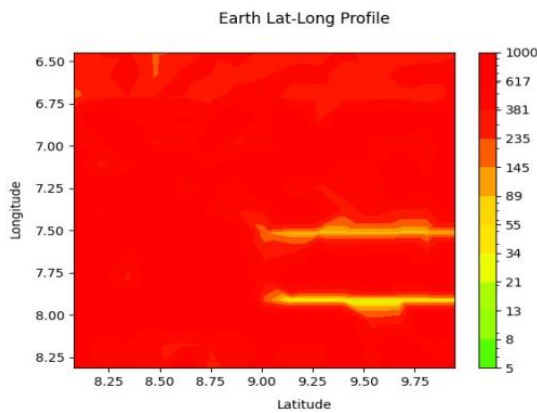


Figure 4.4m: showing Earth Latitude-Longitude Profile

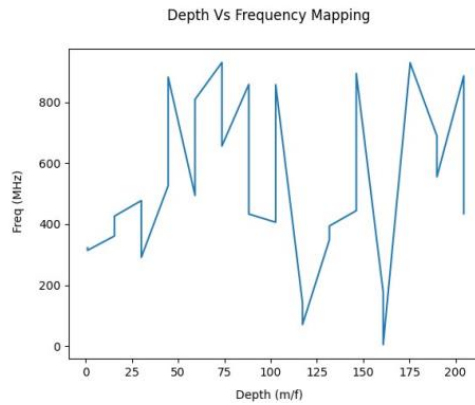


Figure 4.5m: showing Depth versus Frequency Mapping

3D Mapping:Surface-Depth-Frequency

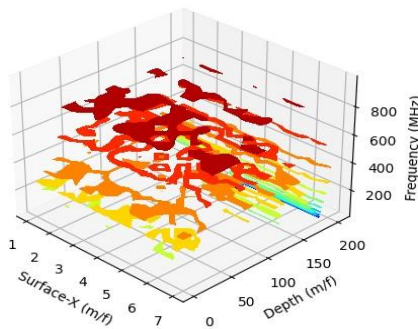


Figure 4.2n: showing 3D Mapping: Surface - Depth –Frequency

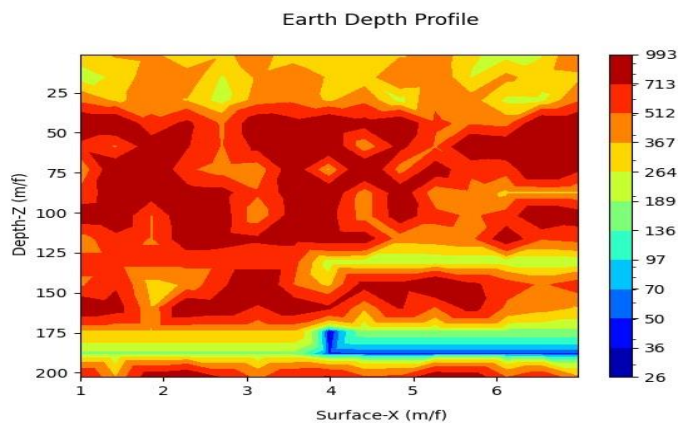


Figure 4.3n: showing Earth Depth Profile

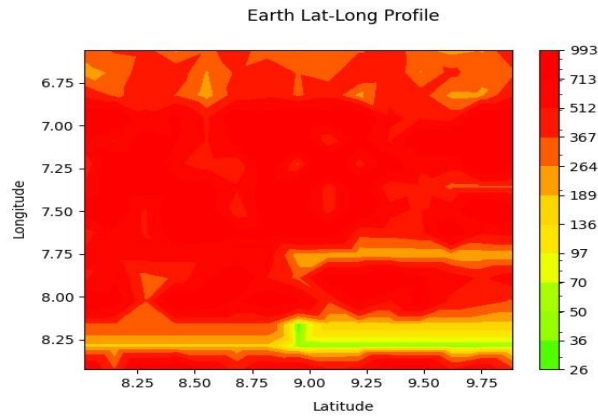


Figure 4.4n: showing Earth Latitude-Longitude Profile

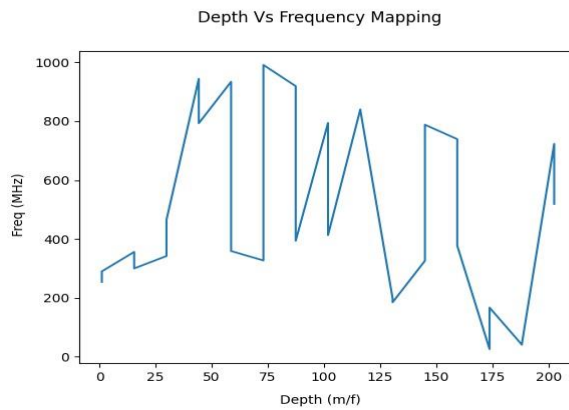


Figure 4.5n: showing Depth versus Frequency Mapping

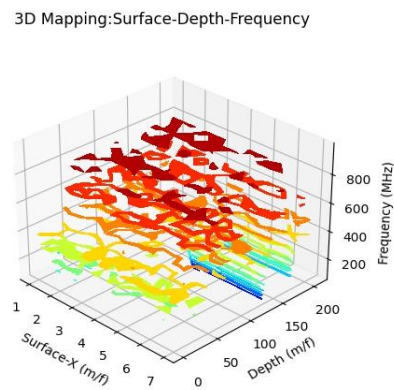


Figure 4.2o: showing 3D Mapping: Surface - Depth -Frequency

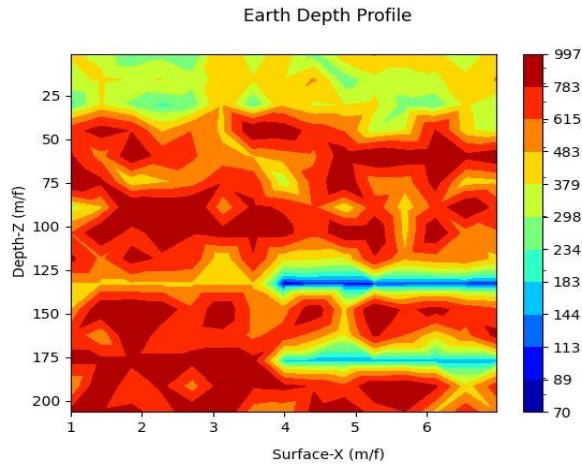


Figure 4.3o: showing **Earth Depth Profile**

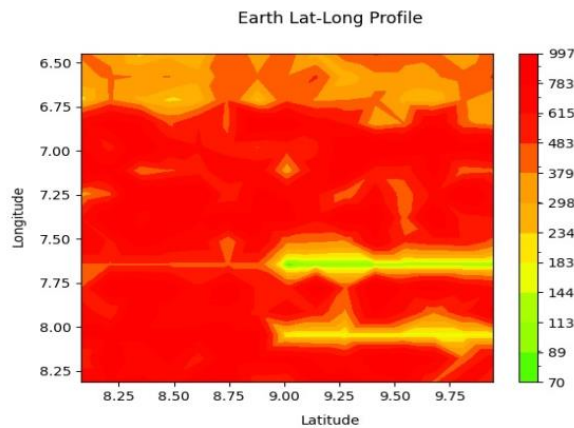


Figure 4.4o: showing **Earth Latitude-Longitude Profile**

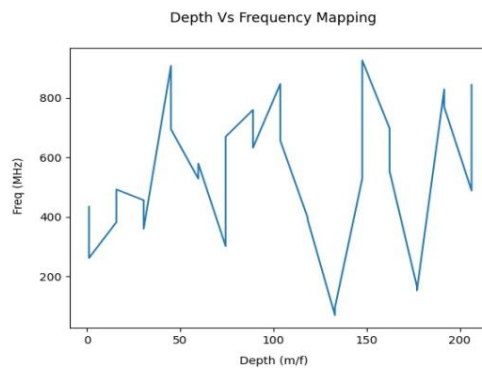


Figure 4.5o: showing **Depth versus Frequency Mapping**

3D Mapping:Surface-Depth-Frequency

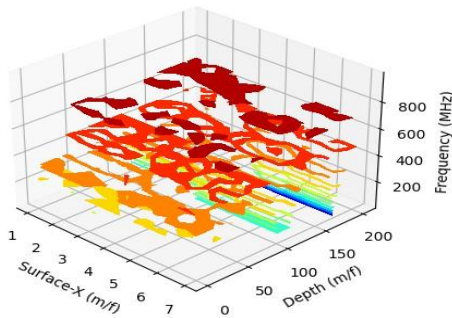


Figure 4.2p: showing 3D Mapping: Surface - Depth –Frequency 7 New

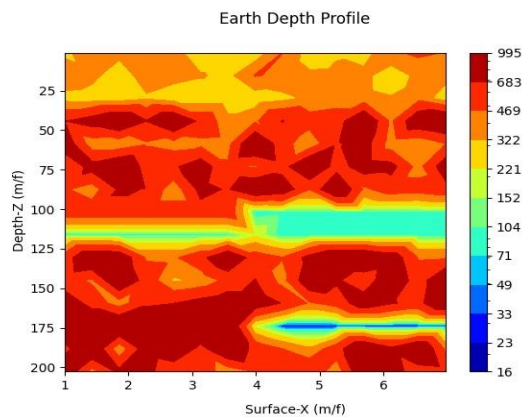


Figure 4.3p: showing Earth Depth Profile 7 New

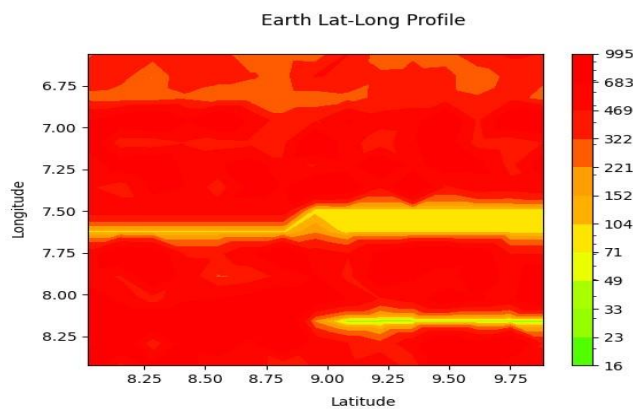


Figure 4.4p: showing Earth Latitude-Longitude Profile 7 New



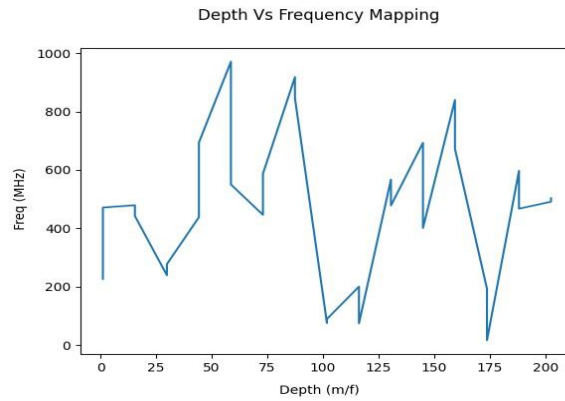


Figure 4.5p: showing Depth versus Frequency Mapping

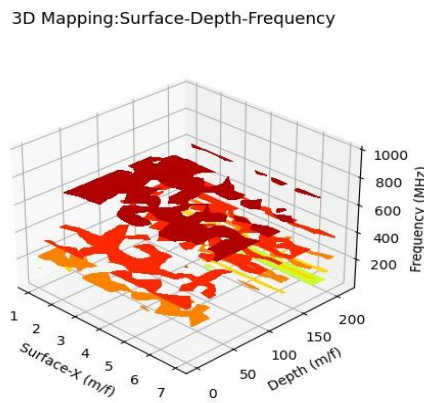


Figure 4.2q: showing 3D Mapping: Surface - Depth –Frequency

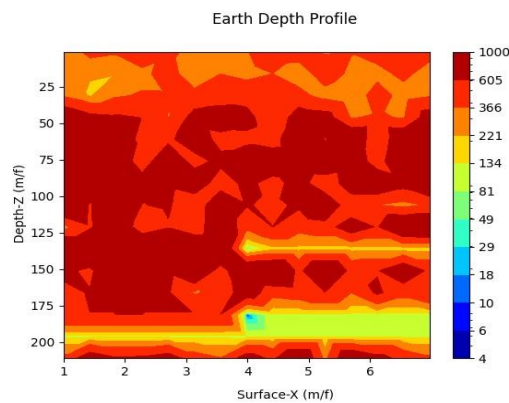


Figure 4.3q: showing Earth Depth Profile

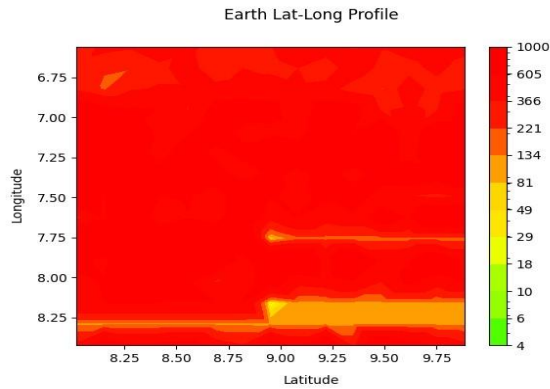


Figure 4.4q: showing Earth Latitude-Longitude Profile

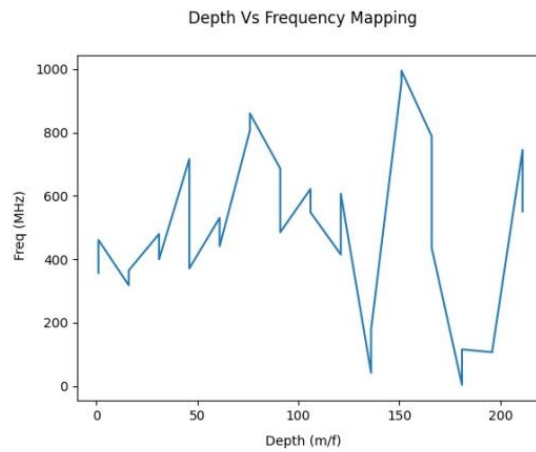


Figure 4.5q: showing Depth versus Frequency Mapping

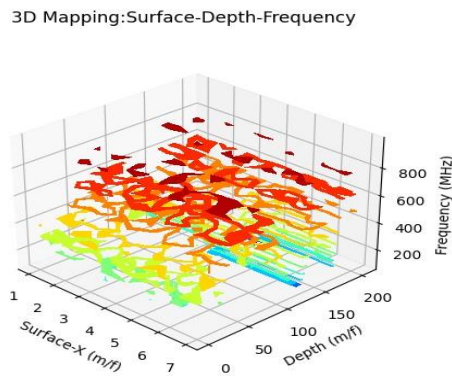


Figure 4.2r: showing 3D Mapping: Surface - Depth -Frequency

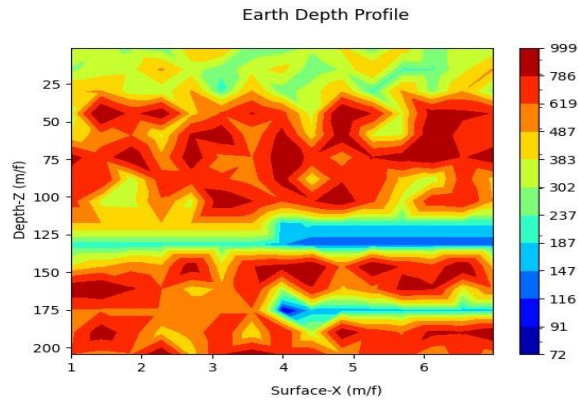


Figure 4.3r: showing Earth Depth Profile

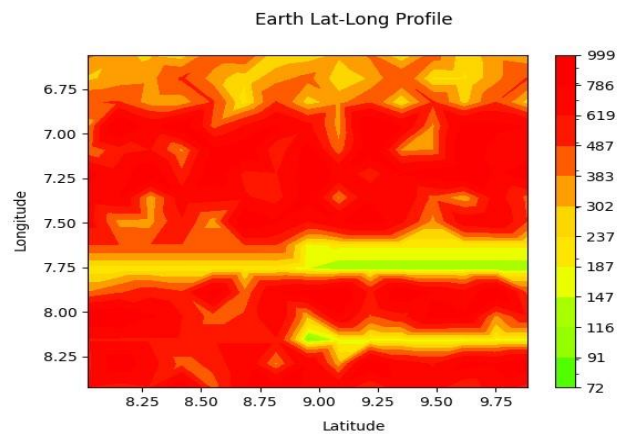


Figure 4.4r: showing Earth Latitude-Longitude Profile

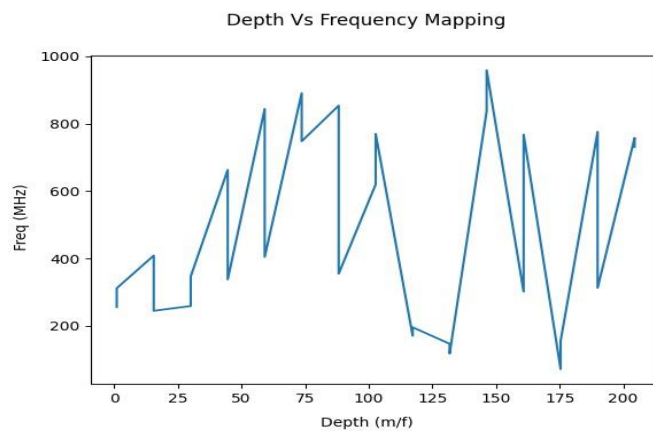


Figure 4.5r: showing Depth versus Frequency Mapping

3D Mapping:Surface-Depth-Frequency

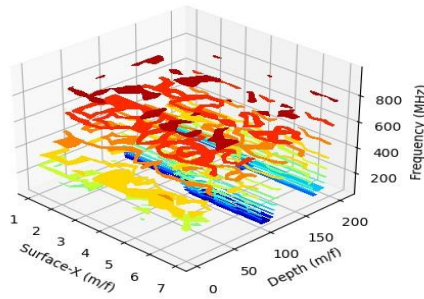


Figure 4.2s: showing 3D Mapping: Surface - Depth -Frequency

Earth Depth Profile

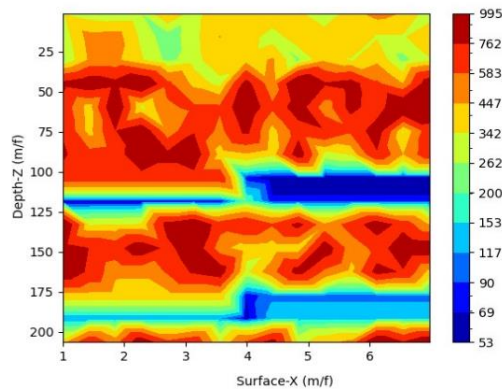


Figure 4.3s: showing Earth Depth Profile

Earth Lat-Long Profile

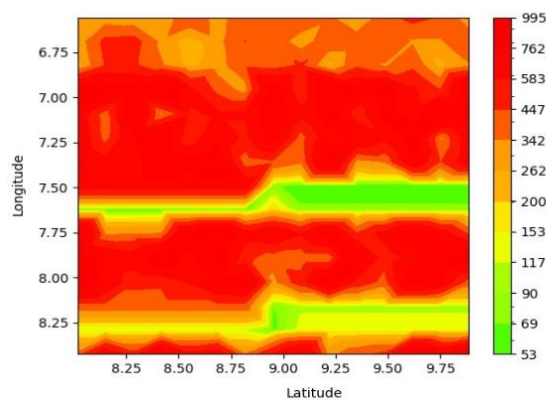


Figure 4.4s: showing Earth Latitude-Longitude Profile

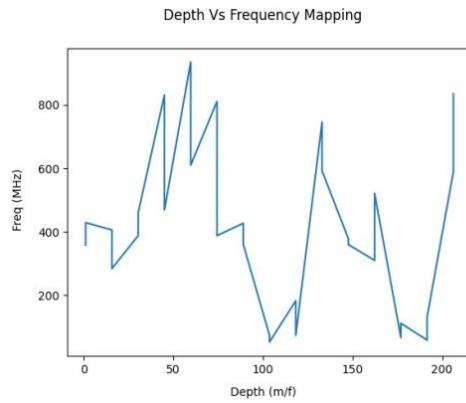


Figure 4.5s: showing Depth versus Frequency Mapping

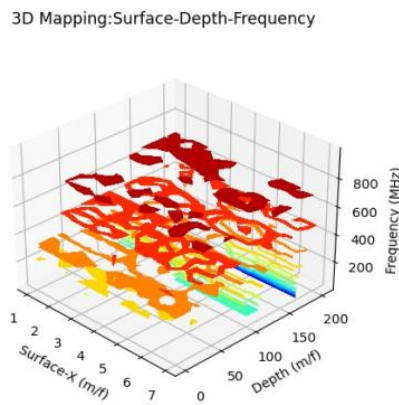


Figure 4.2t: showing 3D Mapping: Surface - Depth –Frequency 7 New

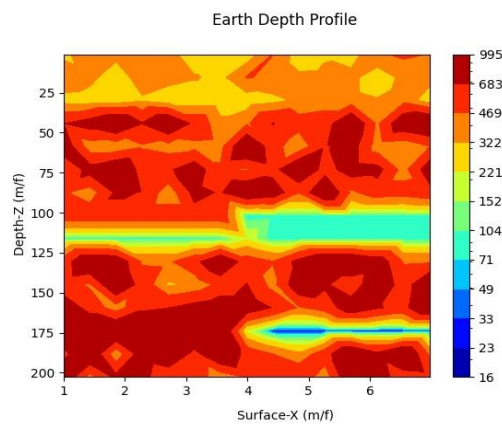


Figure 4.3t: showing Earth Depth Profile 7 New

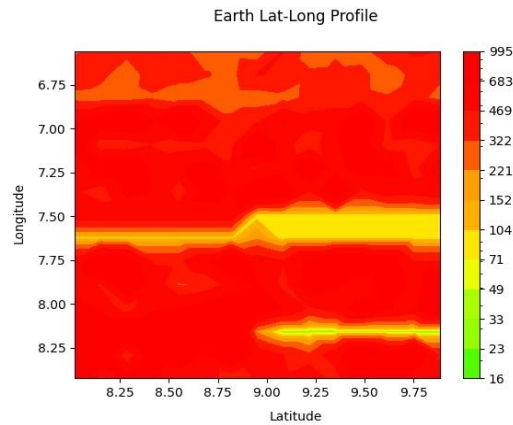


Figure 4.4t: showing Earth Latitude-Longitude Profile 7 New

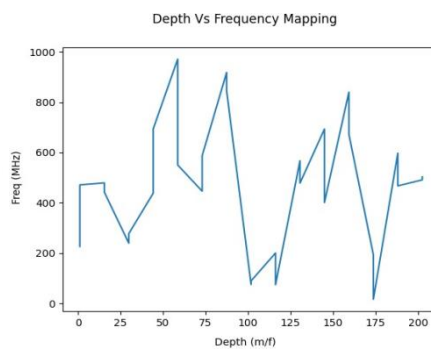


Figure 4.5t: showing Depth versus Frequency Mapping

3D Mapping:Surface-Depth-Frequency

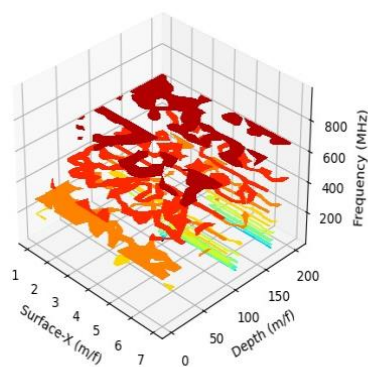


Figure 4.2u: showing 3D Mapping: Surface - Depth –Frequency 7 New

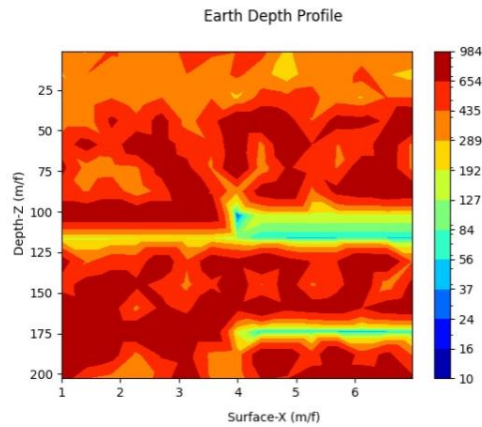


Figure 4.3u: showing Earth Depth Profile 7 New

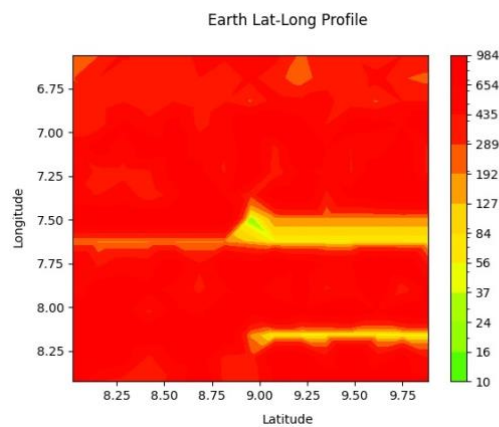


Figure 4.4u: showing Earth Latitude-Longitude Profile 7 New

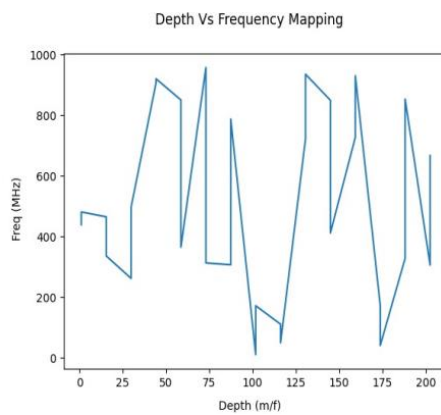


Figure 4.5u: showing Depth versus Frequency Mapping

3D Mapping:Surface-Depth-Frequency

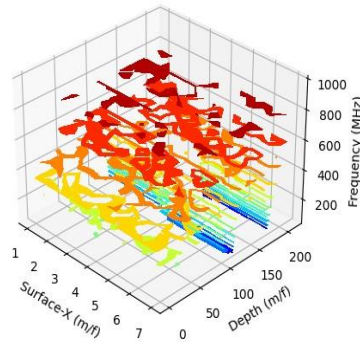


Figure 4.2v: showing 3D Mapping: Surface - Depth –Frequency

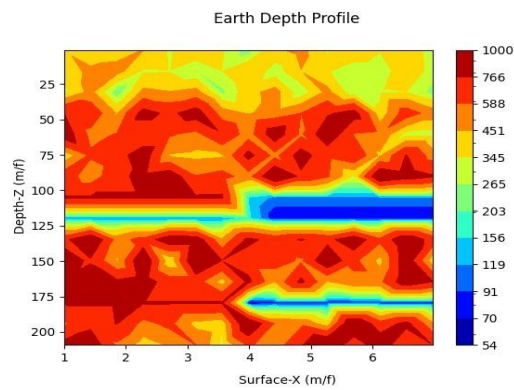


Figure 4.3v: showing Earth Depth Profile

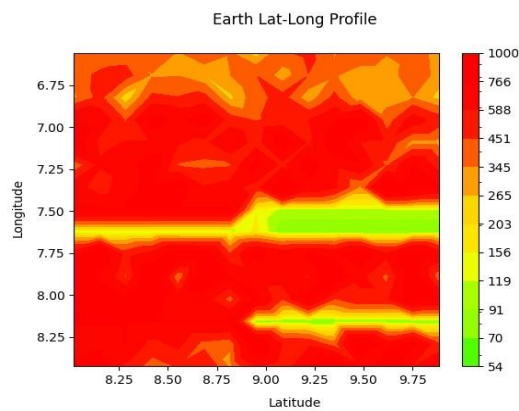


Figure 4.4v: showing Earth Latitude-Longitude Profile

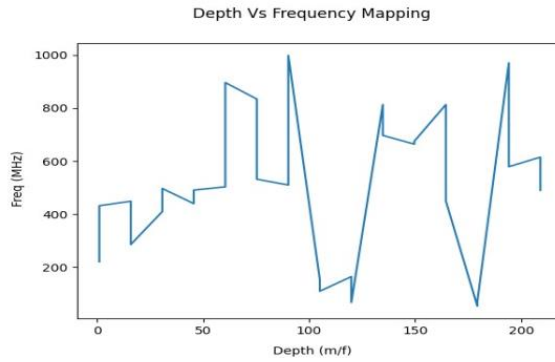


Figure 4.5v: showing Depth versus Frequency Mapping

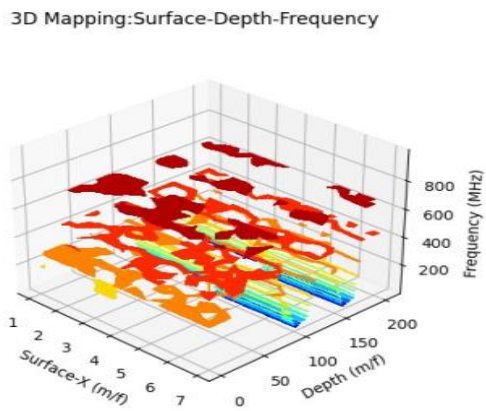


Figure 4.2w: showing 3D Mapping: Surface - Depth –Frequency

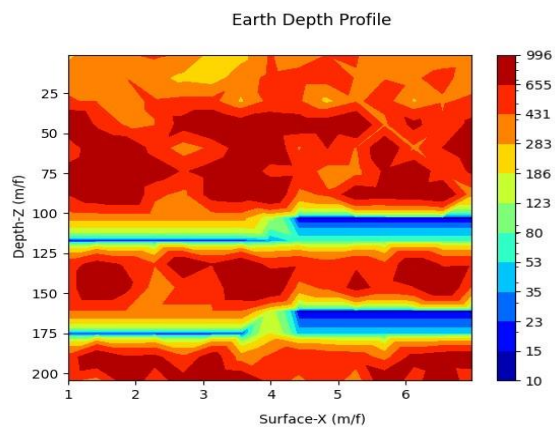


Figure 4.3w: showing Earth Depth Profile

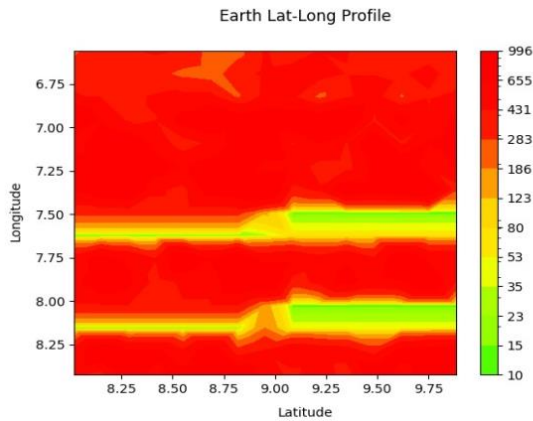


Figure 4.4w: showing Earth Latitude-Longitude Profile

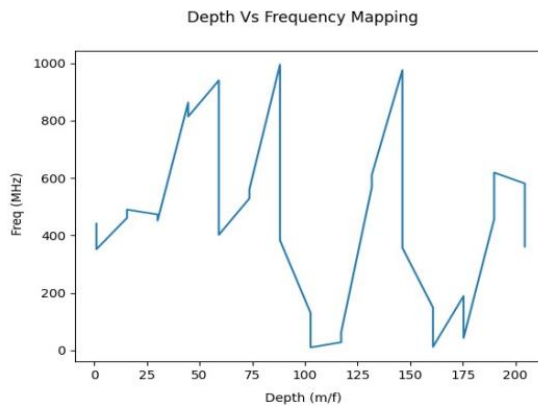


Figure 4.5w: showing Depth versus Frequency Mapping

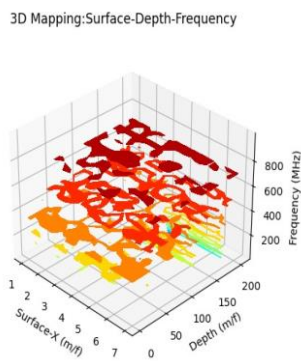


Figure 4.2y: showing 3D Mapping: Surface - Depth –Frequency

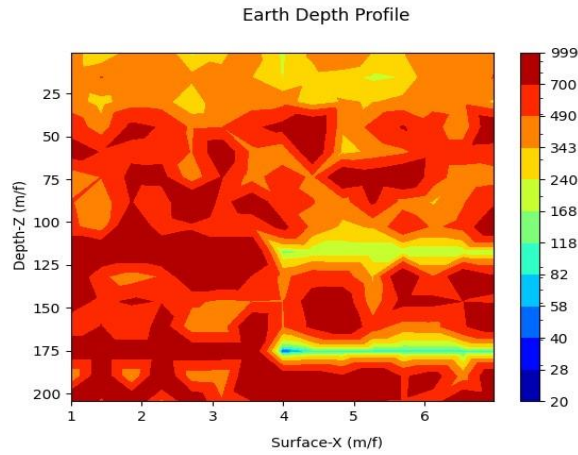


Figure 4.3y: showing Earth Depth Profile

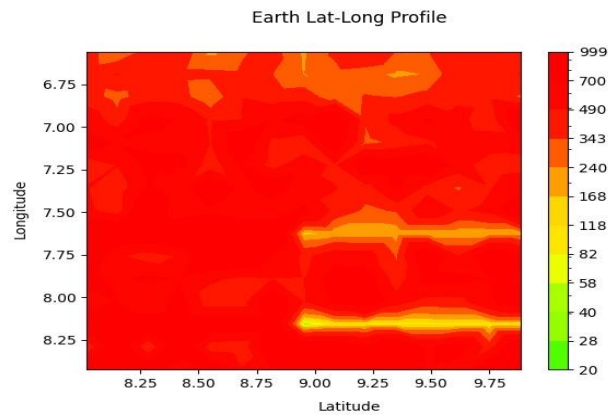


Figure 4.4y: showing Earth Latitude-Longitude Profile

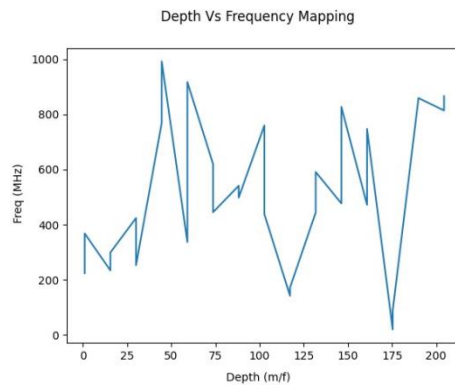


Figure 4.5y: showing Depth versus Frequency Mapping

3D Mapping:Surface-Depth-Frequency

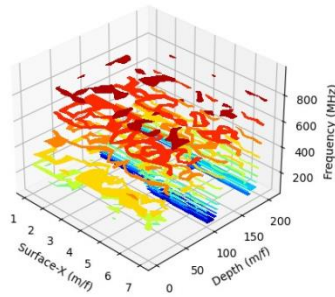


Figure 4.2 BH1: showing 3D Mapping: Surface - Depth –Frequency

Earth Depth Profile

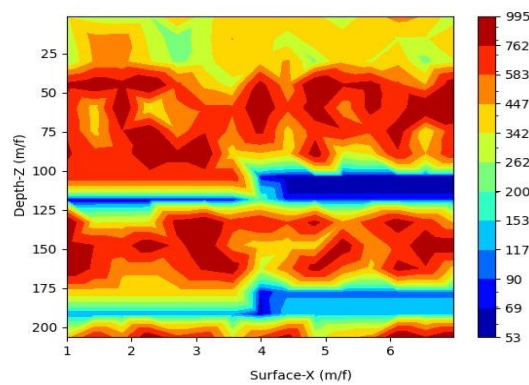


Figure 4.3 BH1: showing Earth Depth Profile

Earth Lat-Long Profile

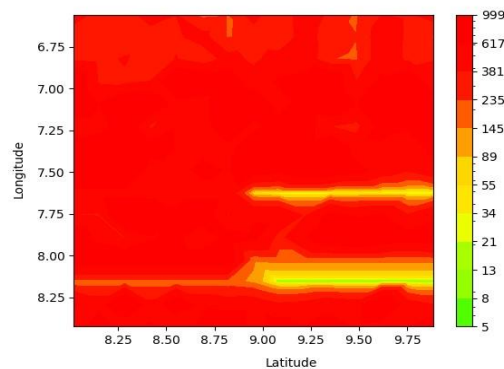


Figure 4.4 BH1: showing Earth Latitude-Longitude Profile

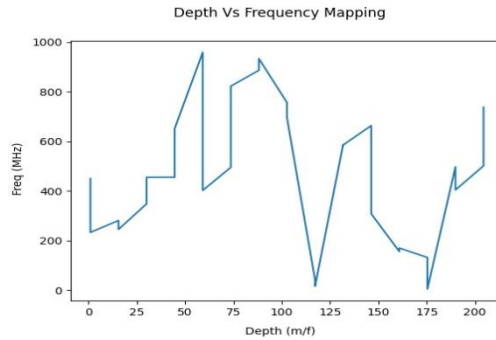


Figure 4.5 BH1: showing Depth versus Frequency Mapping

3D Mapping:Surface-Depth-Frequency

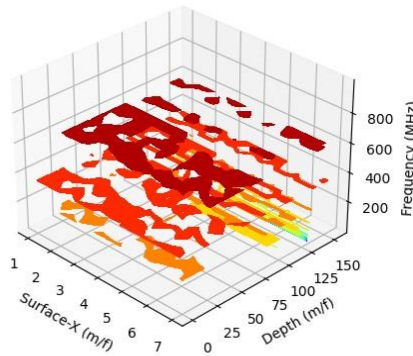


Figure 4.2 BH2: showing 3D Mapping: Surface - Depth –Frequency

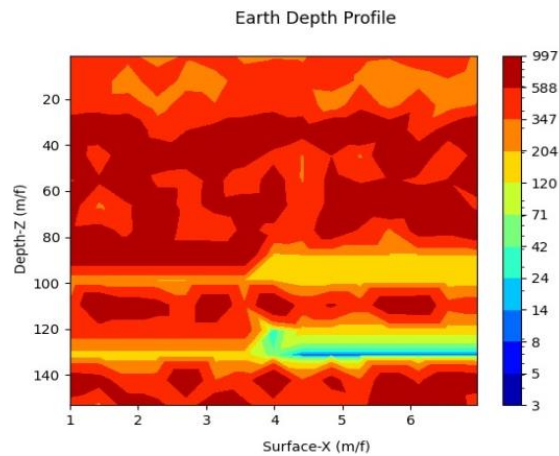


Figure 4.3 BH2: showing Earth Depth Profile

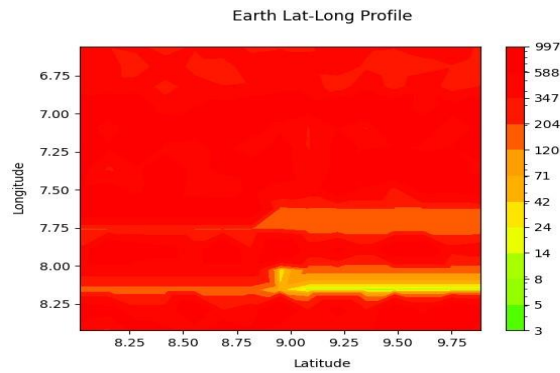


Figure 4.4 BH2: showing Earth Latitude-Longitude Profile

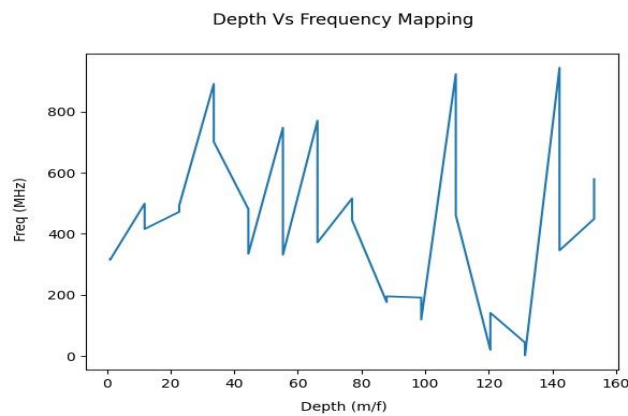


Figure 4.5 BH2: showing Depth versus Frequency Mapping

3D Mapping:Surface-Depth-Frequency

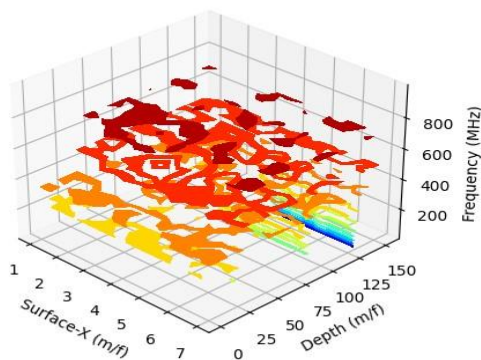


Figure 4.2 BH3: showing 3D Mapping: Surface - Depth –Frequency

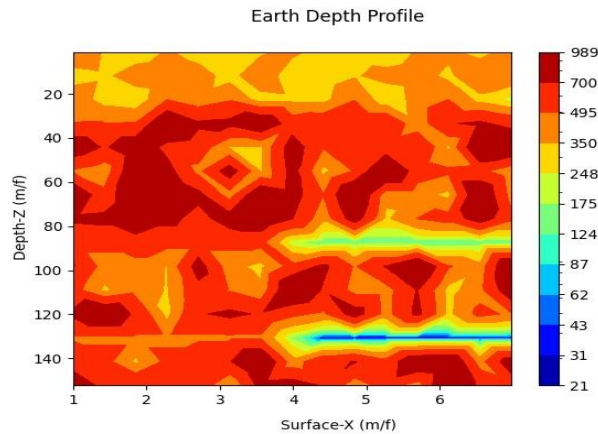


Figure 4.3 BH3: showing Earth Depth Profile

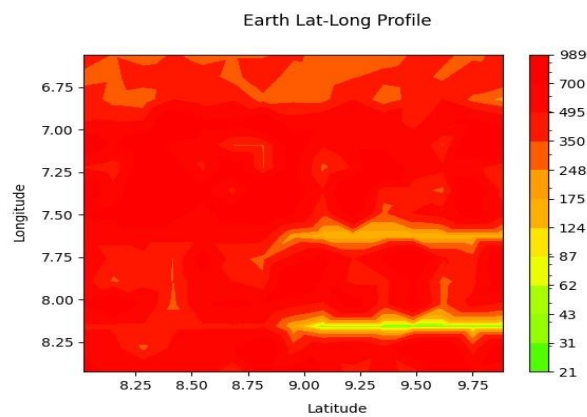


Figure 4.4 BH3: showing Earth Latitude-Longitude Profile

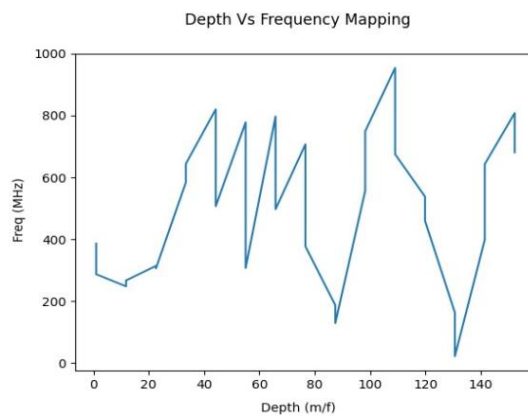


Figure 4.5 BH3: showing Depth versus Frequency Mapping

Table 4.1: Structural traps for sounding points

Sounding point	Structural trap 1(m)	Structural trap 2	Structural trap 3	Borehole Drill Depth (m)
1	108.16	145.6	199.68	219.68
2	98.11	174.4	204.92	216.20
3	103.39	158.25	192.01	214.12
4	97.98	161.88	204.48	222.35
5	95.85	168.27	198.09	211.7
6	99.36	168.48	205.2	227.36
7	99.36	157.68	211.68	216.56
8	101.52	172.8	209.52	231.68
9	123.54	: 157.62	200.22	211.70
10	128.62	154.78	207.1	218.38
11	104.64	159.14	209.28	227.1
12	108.0	164.16	209.51	218.72
13	104.64	152.6	207.1	229.28
14	118.80	172.8	205.2	229.51
15	118.80	169.4	215.6	222.4
16	99.36	162.0	207.35	214.4
17	99.32	161,12	205.11	214.97
18	115.54	165.68	200.56	218.38

Table of structural traps for Sounding points Continues

Sounding point	Structural Trap 1(m)	Structural Trap 2	Structural Trap 3	Borehole Drill Depth (m)
19	99.0	171.6	200.20	224.60
20	99.36	159.84	203.04	229.53
21	102.58	171.71	205.16	234.08
22	151.96	156.96	200.56	227.10
23	106.82	165.68	198.38	227.1
24 BH1	102.31	134.54	167.41	186.21
25 BH2	112.51	145.11	172.31	179.53
26 BH3	109.71	135.00	176.40	179.53



CONCLUSION

Three distinctive structural traps have been identified in each of the sounding points across the study area; the aforementioned structural traps constituted the source bodies harboring the subsurface groundwater system. The regolith or Overburden tends to vary across the study area. The generated structural traps of the sounding, as shown in Table 4.1, give precise aquifer depth as validated by BH1, BH2 and BH3 because results from BH1 to BH3 gave near-perfect structural depth, which could be attributed to aquifer depth with high precision.

REFERENCES

- Akinde A S, Adepelumi A A and Dikedi P N. (2019)..Ifewara Mylonite: Identifying Neotectonic Overprint Using Integrated Geophysical Methods. *J, Geol Geophys*, Vol. 8 Iss 2 No 258
- Alan D. C. and Alan G. J. (2012). The magnetotelluric method: theory and practice. *Cambridge University Press*
- Alsharhan A. S. (1997). Sedimentary basin and petroleum geology of the Middle East, Faculty of Science, UAE University. British Library Cataloguing in Publication
- Cagniard L. (1953). Basic theory of the magnetotelluric method of geophysical prospecting. *Geophysics* Vol. 18, pages 605-635,
- Offodile, M. E. (1992): *An Approach to Groundwater Study and Development in Nigeria*, Mecon Services Ltd. Jos. Pp224-227
- Oliver Ritter, Andreas Junge, Graham J. K. (1998). New Equipment and Processing for magnetotelluric remote reference observation. *Geophysical Jour. Int'l* 132 (3),
- Spitz S. (1985). The Magnetotelluric impedance tensor properties with respect to rotation. *Geophysics* Vol. 50, 1610-1719